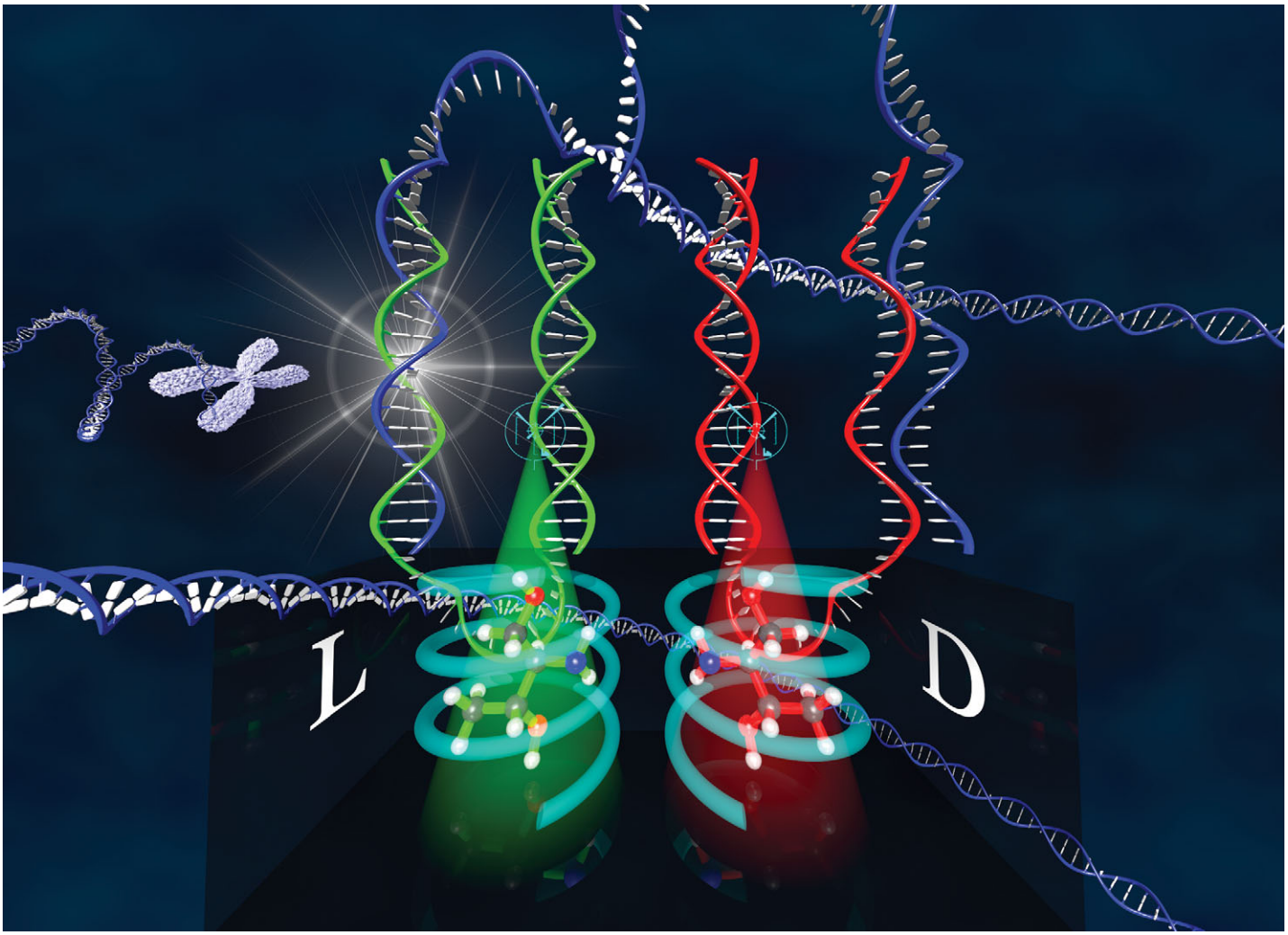

Showcasing research from Asanuma's Laboratory/Department of Molecular Design and Engineering, Nagoya University, Furo-cho, Chikusa-ku, Nagoya, Japan

Acyclic L-threoninol nucleic acid (L-*a*TNA) with suitable structural rigidity cross-pairs with DNA and RNA

Acyclic L-threoninol nucleic acid (L-*a*TNA) hybridizes with DNA and RNA, whereas its enantiomer (D-*a*TNA) does not. This favourable hybridization ability of L-*a*TNA could be attributed to a helical preference for right-handed winding, which is induced by the L-threoninol backbone.

As featured in:

See Hiromu Kashida, Hiroyuki Asanuma *et al.*, *Chem. Commun.*, 2015, **51**, 6500.

ROYAL SOCIETY OF CHEMISTRY

www.rsc.org/chemcomm

Registered charity number: 207890

ChemComm

COMMUNICATION

View Article Online
View Journal | View Issue

Cite this: *Chem. Commun.*, 2015, **51**, 6500

Received 19th November 2014,
Accepted 5th January 2015

DOI: 10.1039/c4cc09244a

www.rsc.org/chemcomm

Acyclic L-threoninol nucleic acid (L-*a*TNA) with suitable structural rigidity cross-pairs with DNA and RNA†

Keiji Murayama, Hiromu Kashida* and Hiroyuki Asanuma*

We report the hybridization properties of a novel artificial nucleic acid: *acyclic* L-threoninol nucleic acid (L-*a*TNA). L-*a*TNA formed a more stable duplex with DNA and RNA than either D-*a*TNA or serinol nucleic acid (SNA) as the rigidity of the L-form was more optimal for interaction with natural nucleic acids.

A number of artificial nucleic acids (XNAs) have been synthesized as mimics of natural DNA and RNA.[1] Locked (bridged) nucleic acids (L(B)NAs)[2] and peptide nucleic acids (PNAs)[3] are examples of XNAs that have high affinities for natural DNA and RNA. These artificial nucleotides are used in various biological applications including RNA silencing[4] and as diagnostic probes and research reagents.[5,6] Recently, XNAs with flexible acyclic scaffolds have attracted attention because the significant difference between acyclic scaffolds and natural ribose or deoxyribose rings affords nuclease resistance in cells.[7–10] However, most XNAs designed from acyclic scaffolds do not form stable homo- or hetero-duplexes with DNA or RNA due to the significant entropy cost to form these duplexes. Only acyclic XNAs that have neutral backbones without phosphodiester linkages, such as PNAs and their derivatives, form tight complexes with natural nucleic acids.[3,11,12] However, the hydrophobicity of these neutral XNAs results in poor solubility in water, and these XNAs are prone to aggregation. In addition, due to the hydrophobic nature of these XNAs their binding to proteins has proven to be problematic. Hence, acyclic XNAs with phosphodiester linkages that can stably cross-pair with natural DNA and RNA are desired.

Meggers *et al.* demonstrated that glycol nucleic acid (GNA), constructed on an acyclic glycol scaffold with phosphodiester linkages, forms stable homo-duplexes despite its flexibility.[13]

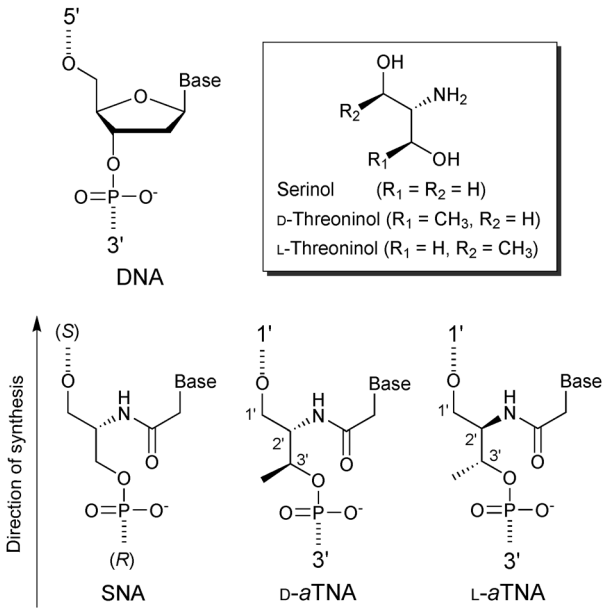

Fig. 1 Structures of artificial nucleic acids synthesized from acyclic diols.

Inspired by this pioneering work, we have developed two novel XNAs: acyclic D-threoninol nucleic acid (D-*a*TNA) and serinol nucleic acid (SNA), shown in Fig. 1.[14–16] Although incorporation of SNA or *a*TNA monomers into DNA or RNA was reported previously, the duplex was severely destabilized.[17,18] In addition, we found that both fully-modified D-*a*TNA and SNA form extremely stable antiparallel homo-duplexes and, interestingly, that SNA stably cross-pairs with DNA and RNA. To the best of our knowledge, SNA is the first fully-modified acyclic XNA with phosphodiester linkages that can recognize both DNA and RNA through base complementarity, and has potential in biological applications.[19] In contrast, D-*a*TNA does not form stable hybrids with either DNA or RNA, although the structural differences between SNA and D-*a*TNA are marginal. We concluded that SNA was flexible enough to conform to DNA or RNA, whereas the methyl group on the D-threoninol scaffold induced rigidity that

Department of Molecular Design and Engineering, Graduate School of Engineering, Nagoya University, Furo-cho, Chikusa-ku, Nagoya 464-8603, Japan.
E-mail: kashida@nubio.nagoya-u.ac.jp, asanuma@nubio.nagoya-u.ac.jp

† Electronic supplementary information (ESI) available: Experimental section containing materials, synthesis and purification of oligonucleotides and results of MALDI-TOF MS, T_m values of L-*a*TNA homo-duplexes, CD spectra of D-*a*TNA/D-*a*TNA and L-*a*TNA/L-*a*TNA, and melting profiles of all L-*a*TNA duplexes. See DOI: 10.1039/c4cc09244a

was unfavourable for hybrid duplex formation.[16] Furthermore, we hypothesized that if *a*TNA could be altered such that it adopted a rigid structure of the "right" conformation, it would form stable duplexes with natural DNA and RNA.

We had believed that D-*a*TNA formed a right-handed helix with complementary D-*a*TNA based on the positive-to-negative Cotton effect at around 240–300 nm (Fig. S1, ESI†).[14,16] We had additionally assumed that L-*a*TNA, synthesized from L-threoninol, an enantiomer of D-threoninol, would not cross-pair with DNA or RNA due to its left-handed helicity. However, several studies on the chiral PNA by the groups of Nielsen and Marchelli[11,20] and by Ly *et al.*[12] showed that the negative-to-positive Cotton effect at around 240–300 nm was due to the right-handed helicity of the chiral PNA/PNA duplex.[20d] Indeed, this chiral PNA forms stable duplex with DNA whereas the hetero-duplex of left-handed PNA was less stable. This assignment suggests that the D-*a*TNA homo-duplex is left handed and that the unfavourable "rigidity" of D-*a*TNA might be due to its propensity to adopt a left-handed helix. This prompted us to examine the cross-pairing of L-*a*TNA with DNA and RNA as we expected that this enantiomer would form a right-handed helix. In this study, we found that L-*a*TNA formed more stable duplexes with both DNA and RNA than SNA due to the more optimal rigidity of the L-*a*TNA.

XNAs synthesized for this study are listed in Schemes 1 and 2. Here, we define the direction of the sequence (indicated by the arrows in Fig. 1, Schemes 1 and 2) as the direction of the elongation reaction of the phosphoramidite monomer on a solid support. **XN*n*a/XN*n*b** and **XN*n*c/XN*n*d** (where *n* is 8 or 15) are complementary in an antiparallel manner, whereas **XN*n*a/XN*n*c** and **XN*n*b/XN*n*d** are complementary in a parallel manner. Synthesis of L-*a*TNA was performed using the procedure described for D-*a*TNA synthesis[14] and modified to optimize yields as described in the experimental section in the ESI.†

The 8-residue L-*a*TNAs (**L-*a*TN8a** and **L-*a*TN8b**) formed an antiparallel homo-duplex with a melting temperature (T_m) of 58.0 °C; this value is the same, within the experimental error, as the T_m of the D-*a*TNA duplex of the same sequence (Table 1). As we reported previously, D-*a*TNA does not stably cross-pair with either DNA or RNA, whereas SNA cross-pairs with both in an antiparallel manner.[14–16] Interestingly, L-*a*TNA cross-paired with both DNA and RNA in a parallel manner. Both **L-*a*TN8a/DN8c** (Fig. 2, solid red line) and **L-*a*TN8a/RN8c** (solid blue line) exhibited distinct sigmoidal melting curves. In striking contrast, antiparallel combinations (**L-*a*TN8a/DN8b** and **L-*a*TN8a/RN8b**) did not show sigmoidal curves (dashed lines). Similarly, **L-*a*TN8b** cross-paired with **DN8d** and **RN8d** but not with **DN8a** or **RN8a** (Fig. S2, ESI†). As summarized in Table 1, T_ms of **L-*a*TN8a/DN8c** (28.4 °C) and **L-*a*TN8a/RN8c** (41.0 °C) duplexes were about 5 °C higher than those of the corresponding SNA/DNA (**SN8d/DN8c**; 23.5 °C) and SNA/RNA (**SN8d/RN8c**; 35.0 °C) hetero-duplexes. Other parallel combinations of 8-residue oligonucleotides showed the trends of duplex stability: hetero-duplexes of L-*a*TNA with DNA or RNA were more stable than those of SNA with the same DNA or RNA strands by 4.4 to 5.7 °C (Table 1).

Table 1 Melting temperatures of the XNA duplexes with eight base pairs

Duplex	Strand orientation	T_m[a]/°C (ΔT_m with SNA)
L-*a*TN8a/L-*a*TN8b	Antiparallel	58.0
D-*a*TN8a/D-*a*TN8b	Antiparallel	58.1[c]
L-*a*TN8a/DN8c	Parallel	28.4 (+4.9)
L-*a*TN8b/DN8d	Parallel	25.6 (+4.4)
L-*a*TN8a/RN8c	Parallel	41.0 (+6.0)
L-*a*TN8b/RN8d	Parallel	37.9 (+5.7)
L-*a*TN8a/DN8b	Antiparallel	—[b]
L-*a*TN8b/DN8a	Antiparallel	—[b]
L-*a*TN8a/RN8b	Antiparallel	—[b]
L-*a*TN8b/RN8a	Antiparallel	—[b]
DN8c/DN8d	Antiparallel	29.0[c]
SN8d/DN8c	Antiparallel	23.5[c]
SN8c/DN8d	Antiparallel	21.2[c]
RN8c/RN8d	Antiparallel	38.9[c]
SN8d/RN8c	Antiparallel	35.0[c]
SN8c/RN8d	Antiparallel	32.2[c]
SN8d/DN8b	Parallel	—[b,c]
SN8c/DN8a	Parallel	—[b,c]
SN8d/RN8b	Parallel	—[b,c]
SN8c/RN8a	Parallel	—[b,c]

[a] Conditions: 2.0 μM oligonucleotide, 100 mM NaCl, 10 mM phosphate buffer (pH 7.0). [b] No sigmoidal curve was observed. [c] Data obtained from ref. 15 and 16.

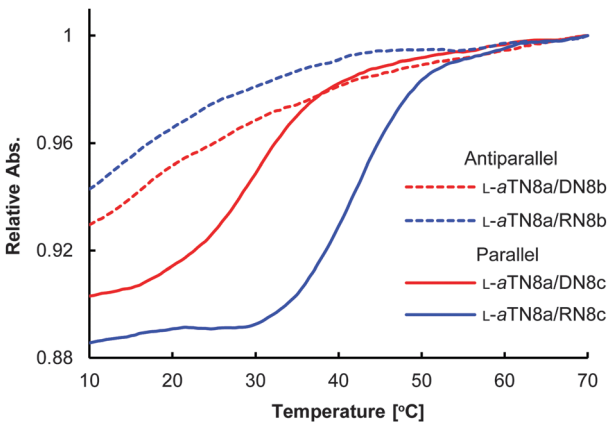

Fig. 2 Melting profiles of the hetero-duplexes of **L-*a*TN8a** with **DN8b** (dashed red line), **DN8c** (solid red line), **RN8b** (dashed blue line), and **RN8c** (solid blue line). Conditions: 2.0 μM oligonucleotide, 100 mM NaCl, 10 mM phosphate buffer (pH 7.0).

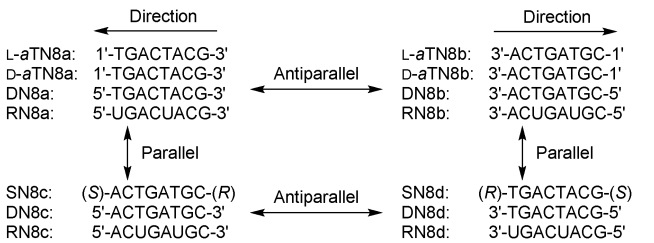

Scheme 1 Sequences of the 8-mer XNAs used in this study. The single-headed arrows indicate the direction of the XNA synthesis. Double-headed arrows show relationships among sequences.

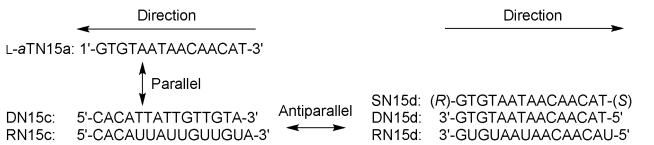

Scheme 2 Sequences of 15-mer XNAs used in this study.

Table 2 Melting temperatures of the XNA duplexes with 15 base pairs

Duplex	Strand orientation	T_m[a]/°C (ΔT_m with SNA)
L-*a*TN15a/DN15c	Parallel	43.7 (+4.5)
L-*a*TN15a/RN15c	Parallel	51.5 (+6.7)
SN15d/DN15c	Antiparallel	39.2[b]
SN15d/RN15c	Antiparallel	44.8[b]
DN15c/DN15d	Antiparallel	47.3[b]
RN15c/RN15d	Antiparallel	49.0[b]

[a] Conditions: 2.0 μM oligonucleotide, 100 mM NaCl, 10 mM phosphate buffer (pH 7.0). [b] Data obtained from ref. 15.

Similar results were also obtained with a 15-nucleotide-long L-*a*TNA. **L-*a*TN15a** cross-paired to form parallel duplexes with **DN15c** and **RN15c** (Fig. S3, ESI† and Table 2). T_ms of these duplexes were also significantly higher than those of the corresponding SNA duplexes by 4.5 to 6.7 °C (Table 2). The stability of the L-*a*TNA/DNA hetero-duplex was comparable to that of the corresponding DNA homo-duplex, and the T_m of the L-*a*TNA/RNA duplex was even higher than that of the corresponding RNA/RNA duplex. Thus, we concluded that L-*a*TNA cross-hybridizes with complementary sequences of both DNA and RNA in a parallel manner irrespective of the sequence, and that the hetero-duplexes are more stable than SNA hetero-duplexes.

L-*a*TNA cross-paired with DNA and RNA only in a parallel manner. This is likely due to the steric configuration at the 2′-amide bond of *a*TNA. SNA cross-pairs with natural oligonucleotides in an antiparallel manner. As shown in Fig. 3a, in an antiparallel hetero-duplex, the 2′-amide bond of SNA protrudes behind the plane of the page enabling formation of hydrogen bonds between the base of the SNA residue and the base of the DNA or RNA. When an L-*a*TNA is antiparallel to a natural nucleic acid strand, the 2′-amide bond protrudes above the plane of the page, and a base pair cannot form (Fig. 3b). In contrast, in the parallel orientation, the configuration of the 2′-amide bond allows base–base hydrogen bonding (Fig. 3c). Thus, the appropriate chirality of 2′-carbon is essential for the hetero-duplex formation. By this reasoning, the configuration of the D-*a*TNA 2′-amide bond should allow cross-pairing with DNA and RNA in an antiparallel manner (Fig. 3d); however, this pairing was not stable. This demonstrates the importance of the position of the methyl group in *a*TNA. In order to elucidate the effect of the position of the methyl group on the duplex structure, CD spectra were recorded (Fig. 4).

The CD signal of the **L-*a*TN8a/L-*a*TN8b** homo-duplex (Fig. 4a) was opposite to that of the corresponding D-*a*TNA homo-duplex (Fig. S1, ESI†). The L-*a*TNA homo-duplex has a negative band at 270–300 nm and a positive band at 240–270 nm. This result is quite reasonable because the L-*a*TNA homo-duplex is an enantiomer of the D-*a*TNA duplex. This positive-to-negative Cotton effect, which is opposite to that observed for B-type DNA duplexes, has usually been thought to result from left-handed helicity. However, according to the interpretation of CD of the chiral PNA duplex,[12,20] the CD signal of the L-*a*TNA homo-duplex results from the right-handed helicity of the duplex. In the CD spectra of all hetero-duplexes of L-*a*TNA with DNA and RNA below the melting temperatures, we

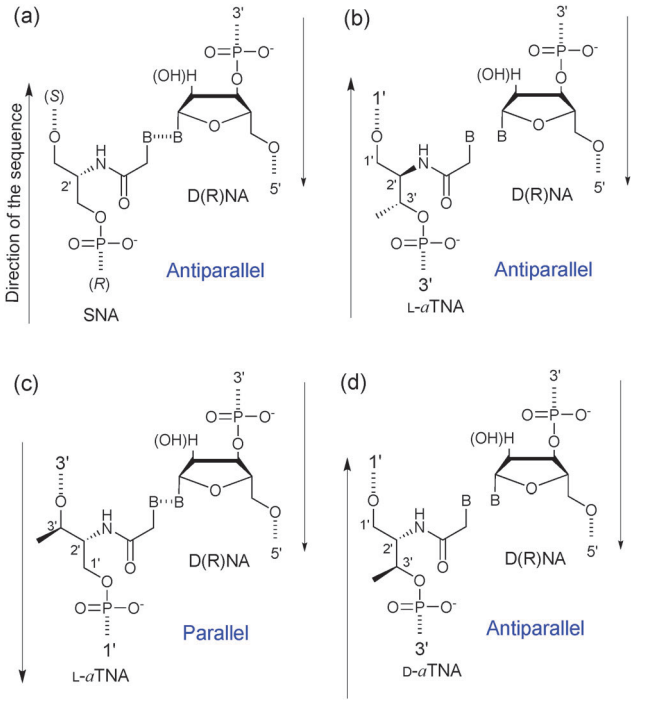

Fig. 3 Relationship between the direction of the sequence and configuration of the 2′-amide bond of SNA and *a*TNA. (a) SNA/D(R)NA in an antiparallel manner. (b) L-*a*TNA/D(R)NA in an antiparallel manner. (c) L-*a*TNA/D(R)NA in a parallel manner. (d) D-*a*TNA/D(R)NA in an antiparallel manner.

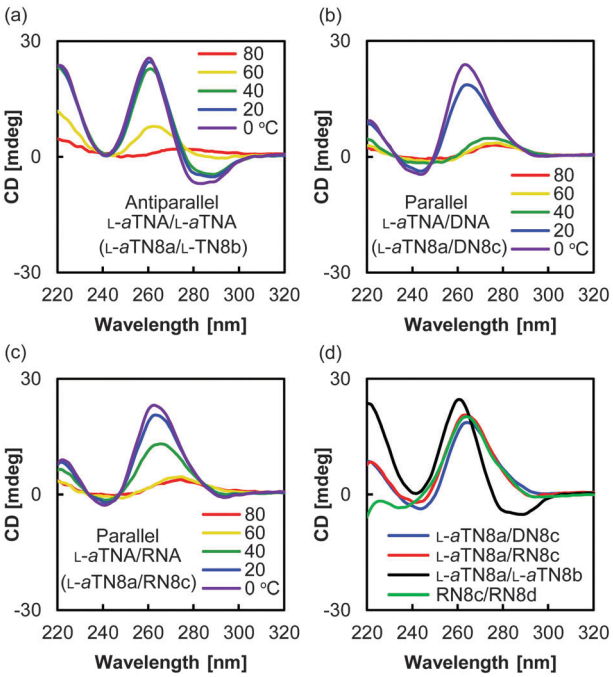

Fig. 4 CD spectra of homo-duplexes of L-*a*TNA and hetero-duplexes of L-*a*TNA with DNA and RNA. Conditions: 4.0 μM oligonucleotide, 100 mM NaCl, 10 mM phosphate buffer (pH 7.0). Spectra of (a) **L-*a*TN8a/L-*a*TN8b**, (b) **L-*a*TN8a/DN8c**, and (c) **L-*a*TN8a/RN8c** recorded at 80, 60, 40, 20, and 0 °C. (d) Spectra of indicated duplexes at 20 °C.

observed a strong positive band at around 260 nm that is characteristic of the right-handed A-form duplex (Fig. 4b–d). Similar A-form-like spectra have also been observed for SNA/DNA and SNA/RNA hetero-duplexes.[16] Previously, we suggested that the flexible acyclic backbone of SNA accommodated to the structures of the DNA and RNA strands.[16] That the L-*a*TNA duplexes have higher T_ms than SNA duplexes may be attributed to the right-handed helicity that is weakly induced in the L-*a*TNA strand by the orientation of the methyl group adjacent to the 2′-amide bond (Fig. 3c). In the case of D-*a*TNA, the methyl group appears to induce left-handed helicity, which prevents cross-pairing with DNA and RNA (Fig. 3d). Our data do not rule out other explanations for the stability of the L-*a*TNA hetero-duplexes. For example, hydrophobicity of the methyl group may stabilize hetero-duplexes with L-*a*TNA or steric hindrance might destabilize D-*a*TNA hetero-duplexes.[21] NMR or X-ray crystal structure analysis will be required to definitively determine the helicity of these duplexes and to evaluate factors affecting duplex stabilities. Further information could also be obtained by analysis of novel XNAs composed of *allo*-threoninol or substituted threoninol.

In conclusion, we have synthesized L-*a*TNA, an enantiomer of previously studied D-*a*TNA. L-*a*TNA has high affinity for DNA and RNA due to the "right rigidity". Hetero-duplexes of L-*a*TNA with DNA and RNA were significantly more stable than SNA hetero-duplexes. L-*a*TNA should find utility in biological applications due to the stability of hetero-duplexes with DNA and RNA and its solubility in aqueous solution. Moreover, this successful example should contribute to further design of novel nucleic acids with well-controlled duplex stability.

This work was supported by a Grant-in-Aid for JSPS Fellows Grant Number (245431) from the Ministry of Education, Culture, Sports, Science and Technology, Japan. The supports by a Grant-in-Aid for Scientific Research (A) (25248037) and The Canon Foundation (for H.A.) are also acknowledged.

Notes and references

1 C. J. Leumann, *Bioorg. Med. Chem.*, 2002, **10**, 841.
2 (*a*) S. Obika, D. Nanbu, Y. Hari, J. Andoh, K. Morio, T. Doi and T. Imanishi, *Tetrahedron Lett.*, 1998, **39**, 5401; (*b*) S. K. Singh, P. Nielsen, A. A. Koshkin and J. Wengel, *Chem. Commun.*, 1998, 455.
3 (*a*) P. E. Nielsen, M. Egholm, R. H. Berg and O. Buchardt, *Science*, 1991, **254**, 1497; (*b*) P. Wittung, P. E. Nielsen, O. Buchardt, M. Egholm and B. Norden, *Nature*, 1994, **368**, 561.
4 (*a*) J. Elmen, M. Lindow, S. Schutz, M. Lawrence, A. Petri, S. Obad, M. Lindholm, M. Hedtjarn, H. F. Hansen, U. Berger, S. Gullans, P. Kearney, P. Sarnow, E. M. Straarup and S. Kauppinen, *Nature*, 2008, **452**, 896; (*b*) R. E. Lanford, E. S. Hildebrandt-Eriksen, A. Petri, R. Persson, M. Lindow, M. E. Munk, S. Kauppinen and H. Ørum, *Science*, 2010, **327**, 198.
5 (*a*) P. E. Nielsen, *Chem. Biodiversity*, 2010, **7**, 786; (*b*) Y. Aiba, Y. Hamano, W. Kameshima, Y. Araki, T. Wada, A. Accetta, S. Sforza, R. Corradini, R. Marchelli and M. Komiyama, *Org. Biomol. Chem.*, 2013, **11**, 5233.
6 (*a*) F. Hövelmann, I. Gaspar, S. Loibl, E. A. Ermilov, B. Röder, J. Wengel, A. Ephrussi and O. Seitz, *Angew. Chem., Int. Ed.*, 2014, **53**, 11370; (*b*) S. Kummer, A. Knoll, E. Socher, L. Bethge, A. Herrmann and O. Seitz, *Bioconjugate Chem.*, 2012, **23**, 2051; (*c*) I. E. Catrina, S. A. E. Marras and D. P. Bratu, *ACS Chem. Biol.*, 2012, **7**, 1586; (*d*) T. Kubota, S. Ikeda, H. Yanagisawa, M. Yuki and A. Okamoto, *Bioconjugate Chem.*, 2011, **22**, 1625.
7 (*a*) K. C. Schneider and S. A. Benner, *J. Am. Chem. Soc.*, 1990, **112**, 453; (*b*) Y. Merle, E. Bonneil, L. Merle, J. Sági and A. Szemzö, *Int. J. Biol. Macromol.*, 1995, **17**, 239.
8 (*a*) P. Nielsen, L. H. Dreiøe and J. Wengel, *Bioorg. Med. Chem.*, 1995, **3**, 19; (*b*) M. A. Campbell and J. Wengel, *Chem. Soc. Rev.*, 2011, **40**, 5680.
9 L. Peng and H.-J. Roth, *Helv. Chim. Acta*, 1997, **80**, 1494.
10 S. Zhang, C. Switzer and J. C. Chaput, *Chem. Biodiversity*, 2010, **7**, 245.
11 S. Sforza, T. Tedeschi, R. Corradini and R. Marchelli, *Eur. J. Org. Chem.*, 2007, 5879.
12 A. Dragulescu-Andrasi, S. Rapireddy, B. M. Frezza, C. Gayathri, R. R. Gil and D. H. Ly, *J. Am. Chem. Soc.*, 2006, **128**, 10258.
13 (*a*) L. L. Zhang, A. Peritz and E. Meggers, *J. Am. Chem. Soc.*, 2005, **127**, 4174; (*b*) E. Meggers and L. Zhang, *Acc. Chem. Res.*, 2010, **43**, 1092.
14 H. Asanuma, T. Toda, K. Murayama, X. Liang and H. Kashida, *J. Am. Chem. Soc.*, 2010, **132**, 14702.
15 H. Kashida, K. Murayama, T. Toda and H. Asanuma, *Angew. Chem., Int. Ed.*, 2011, **50**, 1285.
16 K. Murayama, Y. Tanaka, T. Toda, H. Kashida and H. Asanuma, *Chem. – Eur. J.*, 2013, **19**, 14151.
17 K. S. Ramasamy and W. Seifert, *Bioorg. Med. Chem. Lett.*, 1996, **6**, 1799.
18 V. S. Rana, V. A. Kumar and K. N. Ganesh, *Tetrahedron*, 2001, **57**, 1311.
19 Y. Kamiya, J. Takai, H. Ito, K. Murayama, H. Kashida and H. Asanuma, *ChemBioChem*, 2014, **15**, 2549.
20 (*a*) S. Sforza, G. Haaima, R. Marchelli and P. E. Nielsen, *Eur. J. Org. Chem.*, 1999, 197; (*b*) S. Sforza, R. Corradini, S. Ghirardi, A. Dossena and R. Marchelli, *Eur. J. Org. Chem.*, 2000, 2905; (*c*) V. Menchise, G. De Simone, T. Tedeschi, R. Corradini, S. Sforza, R. Marchelli, D. Capasso, M. Saviano and C. Pedone, *Proc. Natl. Acad. Sci. U. S. A.*, 2003, **100**, 12021; (*d*) T. Tedeschi, S. Sforza, A. Dossena, R. Corradini and R. Marchelli, *Chirality*, 2005, **17**, S196; (*e*) P. E. Nielsen, G. Haaima, A. Lohse and O. Buchardt, *Angew. Chem., Int. Ed.*, 1996, **35**, 1939.
21 A. Gourishankar and K. N. Ganesh, *Artif. DNA: PNA & XNA*, 2012, **3**, 5.